Astron. Astrophys. 326, 741–750 (1997)

ASTRONOMY
AND
ASTROPHYSICS

He I D3 absorption and its relation to rotation and activity in G and K dwarfs⋆

S.H. Saar[1], **J. Huovelin**[2], **R.A. Osten**[1,3], **and A.G. Shcherbakov**[4]

[1] Harvard-Smithsonian Center for Astrophysics, MS 58, 60 Garden St., Cambridge, MA 02138, USA
[2] Observatory and Astrophysics Laboratory, P.O. Box 14 (Tähtitorninmäki), FIN-00014 University of Helsinki, Finland
[3] Center for Astrophysics and Space Astronomy, Campus Box 389, University of Colorado, Boulder, CO 80309, USA
[4] Crimean Astrophysical Observatory, Russian Academy of Sciences, Nauchny, 334413 Crimea, Ukraine

Received 28 November 1996 / Accepted 23 April 1997

Abstract. We have obtained high resolution, high S/N spectra of the He I D3 line (5876 Å) for 53 stars. Combining these data with previous measurements, we investigate correlations between the flux absorbed by D3, $F_{\rm D3}$, rotation and other stellar activity indicators for a set of 76 G and K dwarfs. We find that $F_{\rm D3} \propto P_{\rm rot}^{-1.2}$ for $P_{\rm rot} \geq 4$ days. For $P_{\rm rot} < 4$ days, $F_{\rm D3}$ behaviour depends on spectral type, either remaining roughly constant (G stars), decreasing (K stars), or even going into emission (a few late K stars). We study correlations between D3 and chromospheric (Ca II HK), transition region (C IV 1550 Å) and coronal emission, and find, for $P_{\rm rot} > 4$ days, $F_{\rm D3} \propto \Delta F_{\rm HK}^{1.5}$, $F_{\rm D3} \propto F_{\rm CIV}^{0.7}$, and $F_{\rm D3} \propto F_{\rm X}^{0.6}$, respectively. Thus, D3 has a response intermediate between Ca II HK and C IV in low to moderate activity stars, consistent with its formation in the upper chromosphere. Our data suggest that the maximum flux absorbed by D3 is $F_{\rm D3} \propto T_{\rm eff}^{9.3} \approx 2 \times 10^5$ erg cm^{-2}s^{-1} in G stars (equivalent widths $W_\lambda \leq 80$ mÅ), and about 40% of that value (or $W_\lambda \leq 50$ mÅ) in K stars, less than predicted by current theoretical models. We discuss the implications of our results for stellar activity and He I line formation, and suggest future avenues of study.

Key words: stars: activity – stars: chromospheres – stars: coronae – stars: late-type

1. Introduction

The He I D3 triplet (^{2}P - ^{3}D) at 5875.6 Å has been the subject of recent interest as a diagnostic of stellar magnetic activity because of several useful properties. The very presence of the D3 line in cool stars clearly indicates the presence of non-radiative heating processes, since the line cannot be excited at photospheric temperatures. It shows excellent spatial correlation with solar plages (Landman 1981). The absence of D3 absorption in non-magnetic regions on the sun and other inactive stars suggests that any basal, non-magnetic (e.g., acoustically heated; Schrijver 1995) component to the line is minimal, making it a nearly "pure" magnetic activity signature. D3 absorption is easier to detect against a strong photospheric background than, for example, weak Ca II H and K emission. This property makes it particularly useful for studies of the presence and variability of activity in F dwarfs (Wolff et al. 1985; Garcia López et al. 1993, hereafter GL). Calibration of the D3 line as an activity indicator is, in principle, straightforward, since the only background is the local continuum flux (rather than a model–dependent line core absorption present in most other optical activity diagnostics - e.g., Ca II HK, Hα). The D3 line may also be useful in estimating chromospheric filling factors (Andretta & Giampapa 1995, hereafter AG), Doppler mapping chromospheres on rapid rotators (Piskunov, Huenemoerder, & Saar 1994), and exploring flare activity on active G and K stars (Robinson & Bopp 1987), where the brighter continuum emission makes photometric flare studies difficult.

The exact formation process for D3, however, has been much debated (see reviews in GL and Lanzafame & Byrne 1995). Different investigators have proposed that the He I lines arise via radiative recombination following coronal photoionization (Hirayama 1971; Zirin 1975), via collisional excitation in the dense chromosphere (Athay & Johnson 1960), or some combination of the two (Milkey et al. 1973). Shine et al. (1975) suggest that diffusion of He through strong chromospheric temperature gradients is important (although this is debated by Wolff & Heasley 1984), while Cuntz & Luttermoser (1990) find that formation due to shocks set up by acoustic waves are important in low gravity stars. O'Brien (1980) modelled D3 in the moderately active K2V star ϵ Eri and found coronal "backwarming" to be relatively unimportant. More recently, two independent studies have confirmed this, and extended the result to F and G stars (AG) and active M dwarfs (Lanzafame & Byrne 1995).

Send offprint requests to: S. Saar

⋆ Based in part on observations obtained at the European Southern Observatory, La Silla, Chile, and at the Crimean Astrophysical Observatory, Nauchny, Ukraine

Both groups suggest that the D3 line is primarily collisionally controlled, at least in the non-flaring atmospheres of most cool dwarfs. Neither, however, uses an entirely realistic model for the coronal radiation field.

Nonetheless, D3 line formation in dwarfs is now better understood. Its formation temperature is in the range of 8,000 K $\leq T_{\rm form} \leq$ 40,000 K, with the lower value more typical of the sun and inactive stars, and the latter of more active stars with greater chromospheric column densities (AG). This places D3 at somewhat higher $T_{\rm form}$ than most other optical activity diagnostics, and thus offers a unique probe of the upper chromosphere from the ground. But while several surveys of D3 absorption in dwarfs exist, the total number of measurements is small, except for the F stars (Wolff et al. 1985,1986; Wolff & Heasley 1987; GL). With this in mind, we have undertaken a program to significantly increase the number of D3 measurements on G and K dwarfs. This paper presents the results of the program (some preliminary results based on a much smaller sample were given in Saar et al. 1988 and also reported in Vilhu et al. 1989).

2. Observations and data reduction

Most of the new observations (40) were made with the European Southern Observatory's 1.4m Coudé Auxiliary Telescope with the Coudé Echelle Spectrograph and a cooled RCA CCD detector (512×1024 pixels, each 15 μm square). The data were collected in two observing runs (27 January - 2 February 1988 and 3 - 8 August 1990), and had 100 $\leq$ S/N $\leq$ 300, with typical values of S/N $\approx$ 200. The spectra spanned 40 Å at a resolution $\lambda/\Delta\lambda = 10^5$ with 2.5 pixels per resolution element. All spectra were divided by a flatfield exposure of a tungsten arc lamp to remove pixel-to-pixel sensitivity variations. The flat-fields were very stable over time, with sensitivity changes of less than 0.3% RMS from night to night. Wavelength calibration was accomplished through third order polynomial fits to the positions of 12 to 15 thorium lamp emission lines; RMS deviations between the fitted and measured line positions was typically 0.001Å.

A further 14 spectra were taken at the 2.6 meter telescope of the Crimean Astrophysical Observatory using the University of Helsinki CCD system (Huovelin et al. 1986) with the coudé spectrograph. The CCD system consists of a GEC detector and a CCD 2000 hardware package from Astromed Ltd. (Cambridge, England). The resolution of the system was $\lambda/\Delta\lambda$ = 40,000 as measured by neon comparison lines (0.053 Å/pixel with 3 pixels per resolution element); the average S/N was slightly lower ($\approx$ 150).

We followed the analysis of Danks and Lambert (1985) and divided the target spectra by the spectrum of a rapidly rotating A star in order to remove atmospheric water vapour lines near D3. Like Danks and Lambert, we obtained several high S/N ($\sim$ 400) spectra of the A7Vn star α Pic (HR 2550; $v \sin i$ = 205 km s^{-1}) at various airmasses. Spectra of ESO target stars were either directly divided by one of these (if an α Pic spectrum of nearly the same airmass was available), or by an α Pic spectrum which was scaled to the correct airmass. We required absence of any residual H_2O absorption in the spectrum before the analysis proceeded; in most cases, the correction was small. Identical procedures were used for the Crimean observations, where spectra of α Aql (HR 7557, A7V, $v \sin i$ = 242 km s^{-1}) were used as the comparison for telluric line corrections.

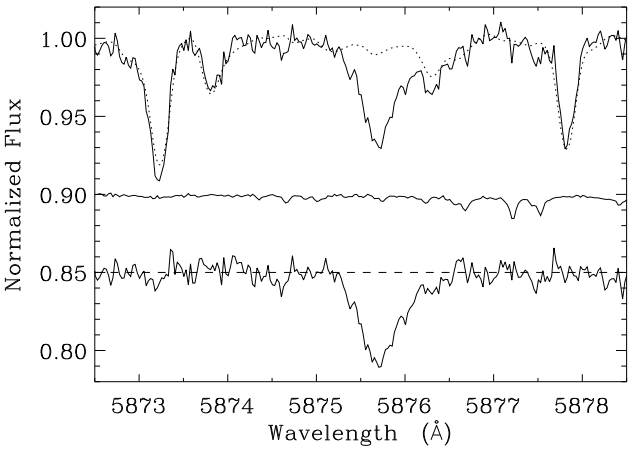

Fig. 1. A sample analysis. The spectrum of the G0V star HD 115383 (upper solid line) is corrected for telluric lines (weak in this case) by dividing by the high S/N spectrum of a rapidly rotating A star (middle solid line), which has been scaled to the same airmass. The spectrum of a G1V comparison star with negligible W_λ(D3), HD 14802 (dotted line), has been corrected for telluric absorption, shifted in λ, broadened to the same $v \sin i$, and scaled slightly to match the radial velocity, the $v \sin i$, and the mean line strengths of HD 115383. Following the subtraction of this modified HD 14802 spectrum to remove line blends, W_λ(D3) is determined from the residual spectrum (lower solid line; pseudocontinuum is dashed).

At this point, we measured the equivalent width (W_λ) of the He D3 line. Typically, D3 is slightly blended by weak, nearby absorption lines, in particular: Fe I 5876.30 Å ($W_{\lambda,\odot}$ = 7 mÅ), Cr I 5876.55 Å ($W_{\lambda,\odot}$ = 4 mÅ), and unidentified lines (blended with H_2O) at 5875.76 Å and 5875.14 Å (Moore et al. 1966). In the (few) cases when the blending appeared to be negligible, we computed the equivalent width directly, after the water vapour correction described above. This value is designated W_λ(D3) in Table 1. Difficulties with blending become significant in the cooler stars and in rapidly rotating stars of all spectral types, and may have caused overestimation of W_λ in some previous measurements. We generally used inactive comparison stars of similar spectral type with no apparent D3 absorption to remove the blends (Fig. 1). The comparison spectrum was convolved with a rotational broadening function (Gray 1988) to match $v \sin i$ and then logarithmically scaled (Marcy 1984) in intensity until the absorption lines in the altered comparison star spectrum matched the line shapes in the target spectrum. In this manner, we approximately accounted for differences in metallicity and $v \sin i$ between the two stars. The altered comparison star spectrum was then shifted to the same radial velocity as the rapid rotator, and subtracted from its spectrum, leaving a residual spectrum with only the D3 line. We then computed W_λ by simple integration of the flux between pseudocontinuum points on either side of the D3 feature. Measurements which have been

derived in this way are designated $W_\lambda^{'}$(D3) in Table 1. We also computed Gaussian fits to the D3 feature, but because D3 is distinctly non-Gaussian in shape at our resolution, the parameters were primarily used only in the error analysis.

Errors in the equivalent width were estimated as follows. The Gaussian fit described above was combined with equations given by Cayrel (1988) to yield an error in W_λ due to noise alone. We also estimated the error due to the uncertainty in the continuum level by redetermining W_λ and and W_λ' after shifting the continuum by $\pm 0.5\sigma_{\rm noise}$. The quadratic sum of these two sources (usually dominated by the error in the continuum level) is given in Table 1. Because of the lower resolution and generally lower S/N, the uncertainty in W_λ(D3) from the Crimean spectra are typically larger than those from the ESO data.

3. Analysis

3.1. Determination of stellar properties and fluxes in D3 and other activity indicators

Rotational periods were derived from Ca II flux modulation (Noyes et al. 1984; Donahue et al. 1996; Baliunas et al. 1996), assumed equal to an binary orbital period (e.g., HD 98230), estimated from the Ca II flux – $P_{\rm rot}$ relationship (Noyes et al. 1984; Soderblom 1985), or in a few cases, estimated from $v \sin i$ assuming an average sin i value and dwarf radius (Saar & Osten 1997). As the latter two methods are less accurate, $P_{\rm rot}$ values from them were given lower weight in subsequent analyses. We have assumed log $T_{\rm eff}$ = 3.908 − 0.234 $(B-V)$ throughout (Noyes et al. 1984). We adopted two convective turnover times: one, $\tau_{\rm C,e}$, empirically derived as the function of $B-V$ which best reduces scatter in the correlation between $P_{\rm rot}$ and normalized Ca II HK flux (Noyes et al. 1984), and the other, $\tau_{\rm C,t}$ (Ossendrijver 1996), derived from theoretical stellar structure models (Kim & Demarque 1996).

We have collected all D3 measurements of G and K dwarfs in the literature. The only D3 measurement not included (to our knowledge) is that of 44 Boo (HD 133604, a F5V + G2V×2 contact binary; Wolff et al. 1985), where it seems likely that the lower limit to W_λ is due to the strong continuum of the inactive primary. Following GL, we have focussed on the flux absorbed by the D3 line as a more physically meaningful quantity than W_λ(D3). To determine $F_{\rm D3}$, we have estimated continuum fluxes for our stars by interpolating from Kurucz (1992) log g = 4.5 models for our adopted $T_{\rm eff}$. We indicate emission in D3 in the figures by giving $F_{\rm D3}$ a negative value. When multiple D3 measurements were available, we have preferentially used those corrected for blends (W_λ'(D3)), with two exceptions. HD 131156A and HD 131511 have W_λ'(D3) values with relatively large errors which also disagree significantly with other measurements. In these cases, we used the average of the W_λ(D3) and W_λ'(D3) measurements.

Finally, we also gathered data on emission in Ca II HK (representing the chromosphere), C IV (1550 Å, representing the transition region), and coronal X-rays for our sample. In the case of Ca II HK, wherever possible we have recomputed the excess Ca II HK flux ($\Delta F_{\rm HK}$) from the original Mount Wilson S values or their equivalent (e.g., Henry et al. 1996), using the calibration of Rutten et al. (1991) to insure a uniform set of $\Delta F_{\rm HK}$ values. For X-ray measurements, we have preferred ROSAT values where available, to reduce any difficulty comparing flux values derived from satellites with different bandpasses. According to our simulations with models in a wide temperature range ($6.2 \leq \log T \leq 7.6$), the only other X-ray data in our sample (from the Einstein IPC) yields flux values differing by less than 10 % from the ROSAT fluxes. Thus, combining data from ROSAT PSPC and Einstein IPC does not cause significant bias in our sample of stars. The final dataset includes 76 G and K dwarfs with 5950 K $\geq T_{\rm eff} \geq$ 3800 K, 45 $\geq P_{\rm rot} \geq$ 0.5 days, spanning -41000 $\leq F_{\rm D3} \leq$ 91000 erg cm^{-2}s^{-1}, a factor of ∼20 in $\Delta F_{\rm HK}$, a factor of ∼300 in $F_{\rm CIV}$, and a factor of ∼2500 in $F_{\rm X}$.

3.2. Comparison with previous measurements

We find reasonable agreement with previous investigators for the 10 stars in common (Fig. 2). There is a small systematic trend such that (excluding HD 165185, see below) $\langle \Delta W_\lambda \rangle$ = $\langle W_\lambda$(D3, this paper) − W_λ(D3, other papers) $\rangle$ = −4.6 ± 3.9 mÅ. We suspect that this is due to the lack of blend correction in previous investigations (save GL). Consistent with this idea, stars with $B-V \leq 0.75$ show (excluding HD 165185) $\langle \Delta W_\lambda \rangle$ = −1.9± 1.5 mÅ, while for the more blended late G and K stars ($B-V > 0.75$), $\langle \Delta W_\lambda \rangle$ = −6.2± 3.9 mÅ. The difference could, however, be partly due to a slight overcorrection for blends on our part. While we think this is unlikely, the small number of stars in common prevents a definitive conclusion.

We note that HD 165185 has an unusually large discrepancy (ΔW_λ = 23 mÅ) despite both D3 measurements being blend corrected. Here we averaged the W_λ'(D3) values to derive the final $F_{\rm D3}$, but we are at a loss to explain the difference in the two results, unless the star varies significantly. This is possible, since HD 165185 is quite active, and possibly quite young, with $\Delta F_{\rm HK}$ lying between that of Hyades supercluster member HD 1835 and Ursa Major stream member HD 39587 (χ^1 Ori).

3.3. Correlations with $T_{\rm eff}$ and rotation

We first examine the relationship between $F_{\rm D3}$ and $B-V$ colour (Fig. 3). We have included the highest $F_{\rm D3}$ measurements from GL in the analysis to extend the range of our dataset in $B-V$. While there is a considerable spread in $F_{\rm D3}$ at any given colour (due to varying levels of activity/rotation), there is a fairly clear upper boundary to $F_{\rm D3}$ given by log $F_{\rm D3} \approx -2.17(B-V)$ + 6.54. Converting colour to $T_{\rm eff}$, this implies a maximum D3 absorption of $F_{\rm D3} \approx 2 \times 10^{-30} T_{\rm eff}^{9.27}$ (erg cm^{-2}s^{-1}) for $0.5 \leq B-V \leq 1.2$. The steep dependence on $T_{\rm eff}$ cannot be due to the conversion from W_λ(D3) to $F_{\rm D3}$ alone, since the continuum flux at D3 goes roughly as $F_{\rm con} \propto T_{\rm eff}^5$ over our range of temperatures (based on a fit to the Kurucz fluxes). Thus, the dependence of the maximum $F_{\rm D3}$ on $T_{\rm eff}$ must at least in part be intrinsic to the behaviour of the D3 line.

Table 1. Stellar parameters, He I D3 measurements, and other activity diagnostics. Numbers in parentheses indicate the number of observations averaged to compute W_λ. D3 references with two numbers are for W_λ and W'_λ, respectively. Helium fluxes F_{D3} are in 10^3 erg cm^{-2}s^{-1}(see text for method); other fluxes (F_{CIV}, ΔF_{HK}, F_X) are in 10^5 erg cm^{-2}s^{-1}.

HD	spec. type	B-V	P_{rot} (d)	P_{rot} ref.	W_λ (mÅ)	W'_λ (mÅ)	D3 ref.	comp. star*	F_{D3}	F_{CIV}	ΔF_{HK}	F_X	flux refs.
Sun	G2V	0.66	25.4	1	≤2	...	1	...	≤4.0	0.09	14.4	0.63	1,2,1
166	K0V	0.75	5.7	2	...	20±4(4)	2c	3	31.2	0.72	44.3	15	3,4,3
1835	G2V	0.66	7.78	3	25	19±4(3)	3,2c	1	40.6	0.86	42.6	12	1,2,5
					...	23±5	2	1	...				
3651	K0V	0.85	44	4	4	...	3	...	4.8	0.04	5.8	0.9	6,2,5
4628	K2V	0.88	38.5	3	...	≤5	2c	2	≤5.6	...	8.3	0.4	2,7
10307	G1.5V	0.62	22	2	<2	...	3	...	<7.9	0.28	10.3	...	1,4
10360	K2V	0.86	35	2	≤4	...	2	...	≤4.7	...	10	1	8,9
10476	K1V	0.84	35.2	3	4	...	3	...	5.0	0.02	7.7	<0.1	3,2,7
10700	G8V	0.72	34	4	≤2	...	4	...	≤3.4	0.02	9.7	0.15	3,2,7
11131	G1V	0.61	5.3	2	...	26 ± 7	2	1	56.3	...	49.3	...	8
13445	K0V	0.82	31	2	...	9 ± 5	2	3	11.8	...	12.7	0.9	8,10
14802	G1V	0.60	19	2	≤4	...	3	...	≤4.4	0.47	10.9	...	1,11
					≤1	...	5	...					
					≤2	...	2	...					
16157	K7Ve+	1.39	1.561	5	...	-185±10	2	5	-41.4	...	...	45	12
17051	G0V	0.56	8.6	2	...	27 ± 12	2	1	65.2	...	32.4	...	8
17084	G5-8V+	0.75	0.955	6	...	32 ± 13	2	2	52.5	...	89.6	250	8,13
17925	K2V	0.87	6.76	3	30	25±3	3,2	3	28.7	0.88	35.0	19	3,2,3
19373	G0V	0.59	18	2	8	...	3	...	18.1	0.1	10.7	0.2	3,4,1
20630	G5Vv	0.68	9.24	3	20.6(9)	20±3(5)	6,2c	2	36.9	0.61	41.8	12	3,2,3
					22	...	5	...					
22049	K2V	0.88	11.68	3	14	...	4	...	19.0	0.39	24.0	5.8	3,2,3
					17.7(12)	...	6	...					
					18	...	5	...					
26965	K1V	0.82	43	4	≤2	...	6	...	≤2.6	0.05	9.1	0.7	3,2,3
30495	G1V	0.63	11	4	20	19±4	5,2	1	39.3	0.68	38.0	9	1,2,5
32147	K4V	1.06	47	4	≤8	...	2	...	≤5.3	...	4.2	≤0.5	2,7
36435	G5V	0.76	11	2	...	19±4	2	1	27.5	...	32.5	...	8
36705	K1V	0.83	0.514	7	...	≤15	8	4	≤19.1	14	81.3	170	1,23,5
38392	K2V	0.94	17	2	...	16±3	2	3	15.1	...	19.0	...	8
39587	G0V	0.59	5.36	3	29	...	6	...	61.1	0.72	50.9	15	3,2,3
					25	...	5	...					
43834	G6V	0.72	32	2	...	≤2	2	2	≤3.4	...	10.2	<1.5	8,14
53143	K0IV-V	0.81	18	2	...	12±2	2	3	16.1	...	22.7	...	8
57853	G0V:	0.59	1.8	8	...	40±7	7	1	90.5	...	55.6	...	15
76151	G3V	0.67	15	4	12	...	5	...	22.7	...	23.9	3.2	2,7
81809	G2V	0.64	40.2	3	6	...	5	...	12.1	...	13.1	0.9	2,7
82558	K2Ve	0.91	1.601	9	...	≤11	8	4	<6.2	3.7	64.1	210	16,17,5
					...	≤6	2	3					
85725	G1V+	0.62	7	10	...	4±2	2	1	8.5	...	...	...	
98230	G5V+	0.66	3.98	11	...	27±9	2c	1	52.2	1.9	59.1	63.0	18,4,11
102365	G5V	0.66	25	2	≤2	...	2	...	3.9	...	11.5	...	8
114613	G3V	0.70	33	2	...	2±2	2	1	3.5	<0.2	7.8	1.2	3,8,3
114630A	G0V	0.60	3.4	2	...	41±7	7	1	90.8	...	59.8	...	8
114630B	G0V	0.60	3.4	2	...	37±9	7	1	81.9	...	59.8	...	8
115383	G0V	0.58	3.33	3	...	33±7	2	1	76.4	1.3	50.0	23	19,2,7
118100	K5Ve	1.18	3.9	12	≤ 20	-12±6	9,2	5	-5.4	2.0	33.8	100	1,20,5
128620	G2V	0.71	29	13	...	≤2	2	1	≤3.4	0.04	8.8	0.09	3,8,3
128621	K0V	0.88	41	2	...	7±4	2	3	7.8	0.05	7.1	0.53	3,8,3
131156A	G8V	0.76	6.31	3	28	21±6	4,2c	2	38.1	0.64	39.6	23	3,2,3
					30	...	3	...					
131156B	K5V	1.17	11.94	3	...	7±7	2c	5	3.3	0.15	14.8	2.3	3,2,3
131511	K1V	0.84	10	2	23	11±8	3,2c	3	21.1	0.42	28.4	6.7	19,21,13
131977	K5V	1.11	27	2	...	10±2	2	5	5.7	...	10.1	3.7	21,22
141004	G0V	0.60	25.8	3	...	≤8	2c	1	≤17.7	0.1	11.1	0.6	3,2,7

Table 1. (continued)

HD	spec. type	B-V	$P_{\rm rot}$ (d)	$P_{\rm rot}$ ref.	W_λ (mÅ)	W'_λ (mÅ)	D3 ref.	comp. star*	$F_{\rm D3}$	$F_{\rm CIV}$	$\Delta F_{\rm HK}$	$F_{\rm X}$	flux refs.
143761	G0V	0.60	17	4	$\leq$3	...	3	...	$\leq$6.6	0.05	10.0	$<$0.3	6,2,7
146233	G2V	0.65	23	2	...	≤ 4	2	1	$\leq$7.9	...	13.0	...	4
147513	G5V	0.64	10	2	...	19$\pm$3	2	1	38.5	...	35.4	...	8
149661	K0V	0.82	21.07	3	14	8$\pm$3	3,2	3	10.5	0.25	19.7	3.8	1,2,7
152391	G8V	0.76	11.43	3	...	16$\pm$9	2c	2	24.4	...	32.2	13	2,7
155885/6	K1Vx2	0.86	20.9	3	...	15$\pm$5	2	2	17.7	0.21	19.0	5.8	3,2,3
156026	K5V	1.16	21	4	...	11$\pm$4	2	5	5.3	...	8.2	1.6	2,7
160269	G0V+	0.60	8.4	2	...	8$\pm$4(2)	2c	1	17.7	...	36.0	5	11,24
165185	G3V	0.62	5.9	2	...	21$\pm$3	2	1	67.8	0.59	46.9	...	25,8
					...	44$\pm$5	10	6					
165341A	K0V	0.86	20	4	20	20$\pm$5	4,2	3	23.6	0.26	19.7	5	3,2,3
185144	K0V	0.79	27	4	13	...	3	...	18.4	0.1	13.9	1.2	3,2,3
186408	G1.5V	0.64	26	2	$\leq$2	...	3	...	$\leq$4.0	...	8.6	...	4
186427	G2.5V	0.66	29	2	$\leq$2	...	3	...	$\leq$3.9	...	7.6	...	4
188088A	K3Ve	1.01	16.5	14	...	22 ± 3	2	5	16.9	...	29.1	6.5	26,13
188088B	K3Ve	1.01	16.5	14	...	26$\pm$3	2	5	20.0	...	29.1	6.5	26,13
190406	G1V	0.61	13.94	3	11	...	3	...	23.8	...	19.1	2.0	2,7
191408	K3V	0.87	45	2	...	≤ 2	2	3	$\leq$2.3	...	5.5	0.3	8,22
192310	K0V	0.88	$>$25	10	...	≤ 2	2	3	$\leq$2.2	...	...	...	
197076	G2V+	0.64	23	2	...	15$\pm$7	2c	1	30.4	...	12.5	...	4
200968	K1Ve+	0.90	16	2	...	8$\pm$2	2	3	8.5	...	21.1	...	4
201091	K5V	1.18	35.37	3	8	$\leq$10(2)	4,2c	5	$\leq$4.5	0.07	6.0	0.6	3,2,3
206860	G0V	0.59	4.86	3	...	30$\pm$5(4)	2c	1	67.9	0.92	52.0	17	1,2,7
209100	K4-5V	1.06	23	2	...	8$\pm$5	2	5	5.3	0.06	12.6	0.6	3,8,3
214953	G0V	0.58	15	2	...	≤ 2	2	1	$\leq$4.6	...	15.9	...	8
216803	K4V	1.10	10.3	15	...	18$\pm$5	2	5	10.5	...	24.0	5.1	8,5
217344	G5Vp+	0.71	1.65	6	...	41$\pm$13	2	2	70.5	...	...	70	13
224930	G2V	0.67	33	4	$\leq$2	...	3	...	$\leq$3.8	...	13.7	0.6	2,7
234677	K4Ve+	1.19	3.85	12	$\leq$20	...	9	...	$\leq$8.7	2.6	45.3	100	27,11,13
283750	K5Ve+	1.12	1.8	16	$\leq$20	...	9	...	$\leq$10.9	5.6	22	160	28,29,13

*Low D3 comparison stars: 1 = HD 14802, 2 = HD 102365, 3 = HD 10360, 4 = HD 22049, 5 = HD 32147, 6 = model

References ($P_{\rm rot}$): [1]Allen (1973); [2]estimated from Ca II; [3]Donahue, Saar, Baliunas (1996), [4]Baliunas, Sokoloff, Soon (1996); [5]Bopp & Fekel (1977); [6]Lloyd-Evans & Koen (1987); [7]Innis et al. (1989); [8]Saar, Nordström, Andersen (1990a); [9]Jetsu (1993); [10]estimated from $v \sin i$ (Saar & Osten 1997); [11],Berman (1931); [12]Pettersen (1989); [13]Hallam et al. (1991); [14]Hooten & Hall (1990); [15]Torres & Ferraz Mello (1973); [16]Olah & Pettersen (1991)

References (D3): [1]Harvey & Livingston (1993); [2]This paper; [2c]This paper (Crimean data); [3]Wolff et al. (1985); [4]Wolff & Heasley (1984); [5]Danks & Lambert(1985); [6]Lambert & O'Brien (1984); [7]Saar et al. (1990a); [8]Vilhu et al. (1989); [9]Pettersen (1989); [10]Garcia Lopez et al. (1993)

References (fluxes): [1]Rutten et al. (1991); [2]Baliunas et al. (1995); [3]Ayres et al. (1995); [4]Duncan et al. (1991); [5]Hempelmann et al. (1995); [6]Baliunas (1996; priv. comm.); [7]Hempelmann et al. (1996); [8]Henry et al. (1996); [9]Stocke et al. (1991); [10]Johnson (1986); [11]Rutten et al. (1989); [12]Caillault (1982); [13]Dempsey et al. (1993); [14]Wood et al. (1994); [15]Pasquini & Pallavicini (1991); [16]Saar (1996, unpublished); [17]Donahue (1996, priv. comm.); [18]Basri et al. (1985); [19]Linsky et al. (1994); [20]Rutten (1987a); [21]Rutten (1987b); [22]Bookbinder (1985); [23]Pasquini et al. (1988); [24]Maggio et al. (1987); [25]Soderblom & Clements (1987); [26]Robinson et al. (1990); [27]Butler et al. (1987); [28]Saar et al. (1990b); [29]Strassmeier et al. (1990)

Correlations of He I D3 with rotation are more complex. In a plot of $F_{\rm D3}$ versus $P_{\rm rot}^{-1}$, a general increase of $F_{\rm D3}$ with rotation rate is evident, at least until $P_{\rm rot} \approx 4$ days (Fig. 4). For shorter periods, the behaviour of $F_{\rm D3}$ is dependent on spectral type: G stars seem to saturate at $F_{\rm D3}$ just under 10^5 erg cm^{-2}s^{-1}, while K stars with $P_{\rm rot} \leq 4$ days show only upper limits to $F_{\rm D3}$, or even D3 in emission. The transition is quite sharp in colour/$T_{\rm eff}$. The dotted line in Fig. 3 connects a sequence of stars in the narrow period range $0.5 \leq P_{\rm rot} \leq 1.8$ days. For $B-V \leq 0.75$, these stars mark the high points of the distribution; for $B-V \geq 0.83$ they are only detected as upper limits, typically at $F_{\rm D3}$ levels *below* detected stars near the same colour which rotate much more slowly. And although the available data is more limited, M dwarfs appear to continue the trend. Slowly rotating, inactive dM stars show no D3 line at all (e.g., GL 15A; Pettersen & Coleman 1981), while dMe flare stars often show D3 in emission

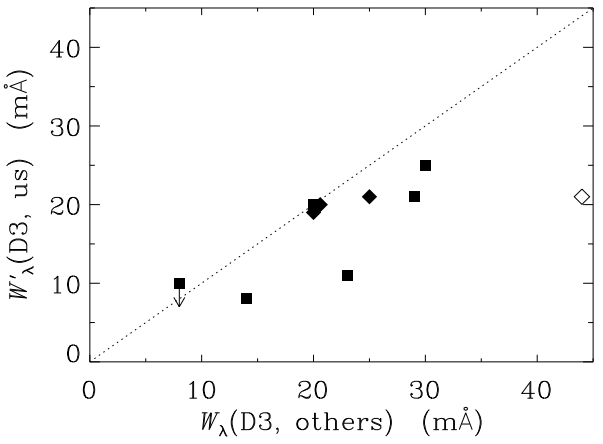

Fig. 2. W'_λ (this paper) versus W_λ(others) in the D3 line for G dwarfs (filled diamonds) and K dwarfs (filled squares). Our measurements tend to show smaller W_λ values, probably due to our correction for blends in the D3 line. Consistent with this, the discrepancy is larger in late-G and K stars where blends are stronger. The highly discrepant point (open diamond) is HD 165185 (see text).

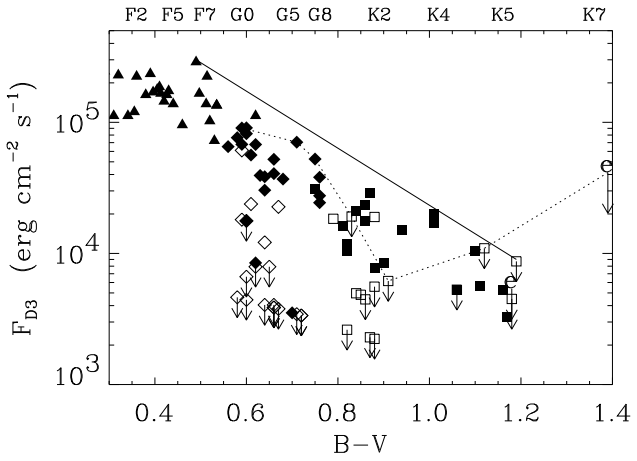

Fig. 3. F_{D3} vs. $B-V$ colour for G (diamonds) and K (boxes) dwarfs (filled symbol if F_{D3} is blend corrected - i.e., from W'_λ(D3) - otherwise an open symbol), plus a selection of high F_{D3} stars (mostly F dwarfs) from GL (triangles). Upper limits are plotted with an open symbol of the appropriate type and a short arrow; K stars with D3 in emission are plotted at $|F_{D3}|$ with an "e" plus a long arrow. Approximate spectral types are shown at the top. An empirical upper bound to F_{D3} for mid-F to late K dwarfs is given by the solid line, equivalent to a maximum flux absorbed by D3 of $F_{D3} \approx 2 \times 10^{-30} T_{\rm eff}^{9.27}$ (erg cm^{-2}s^{-1}) for $0.5 \leq B-V \leq 1.2$. The dotted line connects a sequence of stars with $0.5 \leq P_{\rm rot} \leq 1.8$ days.

(Giampapa et al. 1978; Pettersen et al. 1984; Pettersen 1989) even outside of flares. Thus, for rapid rotators, it appears that D3 flux decreases sharply towards cooler $T_{\rm eff}$, eventually becoming an emission line in active late K and M dwarfs. (We defer a more detailed discussion of D3 in M dwarfs to a future paper.)

A least squares fit to the stars with $P_{\rm rot} \geq 4$ days yields $F_{D3} \propto P_{\rm rot}^{-1.2\pm0.2}$, with the error in the exponent reflecting both the statistical noise and the variation in the power law depending on how the points were weighted (e.g, lower weights on estimated $P_{\rm rot}$ values, lower weights on non-blend corrected F_{D3}, etc.). Use of the Rossby number to characterize rotation does not improve the fits. In fact, it actually increases the scatter significantly (Fig. 5). We have tried both $\tau_{\rm C,e}$ and $\tau_{\rm C,t}$ to construct Rossby numbers, but either leads to $\sim 100\%$ increase in the rms scatter for the fit to the slower rotators.

3.4. Correlation of F_{D3} with other activity fluxes

It is also interesting to investigate the D3 line relative to other activity diagnostics. We show the results for the three emission fluxes we have selected (Ca II HK, C IV 1550 Å, and soft X-ray flux) in Figs. 6, 7, and 8. Due to the strong change in D3 characteristics at short periods (see above, Fig. 4), we have excluded all stars with $P_{\rm rot} < 4$ days from the fit.

Depending on how the data are weighted, we find $F_{D3} \propto \Delta F_{\rm HK}^{1.5\pm0.2}$ (Fig. 6), $F_{D3} \propto F_{\rm CIV}^{0.7\pm0.1}$ (Fig. 7), and $F_{D3} \propto \Delta F_{\rm X}^{0.6\pm0.2}$ (Fig. 8). Thus, F_{D3} acts like a line formed somewhere between Ca II HK and C IV (and closer to C IV), in line with its formation in the upper chromosphere (e.g., AG; Lanzafame & Byrne 1995). As a consistency check, the power law indices derived for F_{D3} are themselves consistent with the relations between Ca II HK, C IV, and X-ray flux derived by Rutten et al. (1991), who found a 1.0:1.9:2.3 ratio between their power law indices. The exponent on the D3 – Ca II HK relation suggests a similarity with the Si II (1808, 1817 Å) lines, supporting the idea that D3 may have a similar average formation height of 10,000 K $\leq T_{\rm form} \leq$ 25,000 K (Rutten et al. 1991).

4. Discussion

The He I D3 line exhibits several interesting characteristics. First, it has a fairly well defined upper limit which scales like $F_{D3} \propto T_{\rm eff}^{9.3}$. This works out to a maximum of $F_{D3} \approx 1.8 \times 10^5$ erg cm^{-2}s^{-1} in a G0 dwarf (or equivalently, a maximum $W_\lambda \approx$ 80 mÅ). The maximum in a K0 dwarf works out to $F_{D3} \approx 6.5 \times 10^4$ erg cm^{-2}s^{-1} ($W_\lambda \approx 50$ mÅ). These values are noticeably less than the maximum estimated for F and G stars by AG. They found a maximum W_λ(D3) $\approx 100 - 150$ mÅ based on their D3 models, as constrained by parallel models of Hα (they required that the latter show residual line core emission $W_\lambda \leq$ 1Å). While AG note that their maximum W_λ is likely an overestimate, without the Hα constraint, their D3 models do not show a maximum D3 value for the range of chromospheric mass loading excess (over the quiet sun), $0 \leq \Delta \log m \leq 1.8$ which they study. As this approximately corresponds to $3.7 \leq \log F_{\rm X} \leq 7.3$, the AG models would seem to cover activity from solar levels to extremely active stars. The fact that they found *no* maximum D3 flux over this range is thus noteworthy. We can think of three possible ways to explain the inconsistency.

1) Dwarfs with the "true" maximum D3 absorption (if such exists) may still be unobserved. While certainly possible, we believe that this explanation is somewhat unlikely. Our dataset

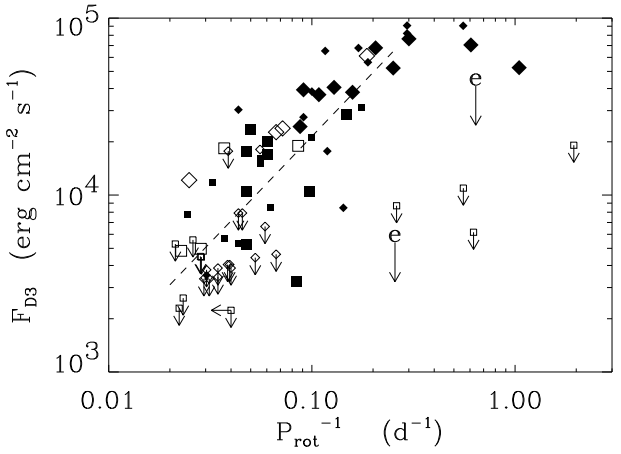

Fig. 4. F_{D3} vs. P_{rot}^{-1}, with symbols as in Fig. 3. For detected D3 lines, a smaller symbol indicates an estimated (rather than directly measured) P_{rot} value. F_{D3} appears to saturate in G stars, and fall to zero (or go into emission) in K stars, for $P_{rot} \leq 4$ days. For $P_{rot} \geq 4$ days, we find $F_{D3} \propto P_{rot}^{-1.2\pm0.2}$, depending on how the data are weighted (dashed line).

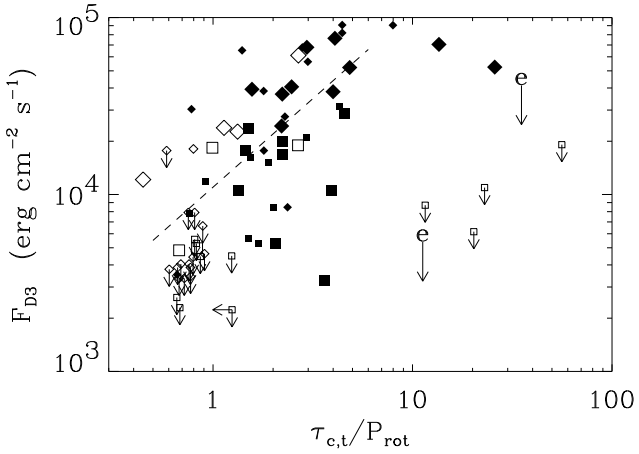

Fig. 5. F_{D3} vs. $\tau_{c,t}/P_{rot}$ (the inverse Rossby number using theoretical τ_c values) with symbols as defined in Fig. 3; smaller symbols denote estimated P_{rot}. A plot using empirical τ_c values is similar. The scatter is considerably larger than for F_{D3} vs. P_{rot} (Fig. 4); best fit is $F_{D3} \propto (\tau_{c,t}/P_{rot})^{1.1\pm0.3}$ for $P_{rot} \geq 4$ days, depending on how the data are weighted (dashed line).

already samples P_{rot} values well into the magnetic activity "saturation" regime ($P_{rot} \leq 3$ days in dwarfs; e.g., Vilhu 1984) over the full range of $B-V$ colour for G and K dwarfs. Thus, if D3 saturates approximately at the same point as most other activity indicators (and it appears to do so, at least in G dwarfs), then our sample should also cover this regime.

2) It may be that the models of AG are incomplete in some way. Lanzafame & Byrne (1995), for example, found that the number of levels included in their model He I atom affected whether D3 appeared in emission or absorption in an active M dwarf. Details of the outer atmospheric structure used in the

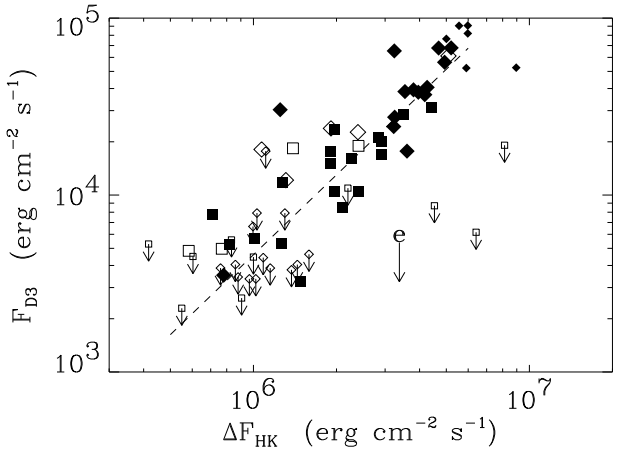

Fig. 6. F_{D3} vs. ΔF_{CaII}, with symbols as defined in Fig. 3. A fit $F_{D3} \propto \Delta F_{CaII}^{1.5\pm0.2}$ for $P_{rot} \geq 4$ days is shown (dashed line).

models, such as the thickness of the "Lyman plateau" (AG) are uncertain. Also, no existing set of models of D3 in cool stars properly treats the coronal EUV radiation. AG scale from quiet solar coronal fluxes, but it is quite likely that as activity increases, the coronal spectrum changes shape (i.e., mean temperature) as well as overall amplitude (e.g., Giampapa et al. 1996). More detailed modelling would be helpful.

3) The third possibility is that the theoretical maximum W_λ(D3) is never reached due to "filling-in" of the line due to some other process, the mostly likely candidate being low-level flaring. Emission in D3 due to flares has been observed in active RS CVn's (e.g., Huenemoerder & Ramsey 1987), dMe stars, and even in one of our targets (HD 20630; Robinson & Bopp 1987). It is possible that frequent, low-level flaring (enough to keep the line partly filled in at all times) could be responsible for preventing the theoretical maximum W_λ(D3) from ever being achieved. Careful monitoring of D3 on an active star for short timescale fluctuations could test this idea. The D3 line may turn out to be useful as a diagnostic of flare characteristics in F, G, and K stars, whose strong optical continua render photometric monitoring of flares mostly fruitless.

For G dwarfs, our maximum W_λ is actually quite consistent with the maximum non-flaring solar chromosphere value ($W_\lambda \approx$ 80 mÅ; AG). This suggests that a G dwarf with saturated activity levels is basically covered over its entire surface with the most active plage seen on the sun. Along these lines, using our value for the maximum W_λ(D3) increases the chromospheric filling factors (A_{D3}) inferred by the method of AG, who found that $A_{D3} \geq W_\lambda$(D3)/ W_λ(D3, max). To pick three well observed examples, we found that $A_{D3} \geq 0.35, 0.33$, and 0.50 for HD 39587 (χ^1 Ori), HD 20630 (κ^1 Ceti), and HD 131156A (ξ Boo A), respectively, using our values for the maximum F_{D3} to calculate W_λ(D3, max) for each star's T_{eff}. These revised A_{D3} values are in better agreement with analogous estimates based on the He I 10830Å line ($A_{10830} \geq 0.45, 0.57$, and 0.40, respectively; AG), whose upper quantum level is the lower level

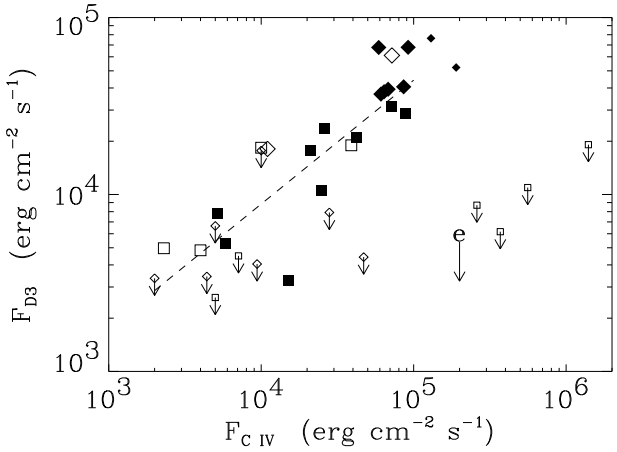

Fig. 7. $F_{\rm D3}$ vs. $F_{\rm CIV}$, with symbols as defined in Fig. 3. A fit $F_{\rm D3} \propto F_{\rm CIV}^{0.7\pm0.1}$ for $P_{\rm rot} \geq 4$ days is shown (dashed line).

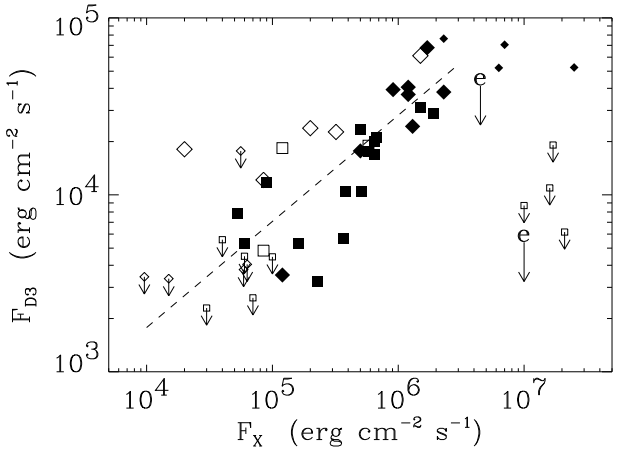

Fig. 8. $F_{\rm D3}$ vs. $F_{\rm X}$, with symbols as defined in Fig. 3. A fit $F_{\rm D3} \propto F_{\rm X}^{0.6\pm0.2}$ for $P_{\rm rot} \geq 4$ days is shown (dashed line).

of D3. The better agreement between A_{10830} and our new $A_{\rm D3}$ values increases confidence in the AG method as a useful tool for probing chromospheric filling factors.

The He I D3 feature is also remarkable in its strongly varied response as a function of $T_{\rm eff}$ in the rapid rotators. While for "unsaturated" stars D3 behaves "normally", increasing in absorption with increasing rotation, and showing consistent correlations with other activity diagnostics, the behaviour clearly diverges once stars become very active. Its behaviour is reminiscent of Hα in cooler M dwarfs (e.g., Cram & Mullan 1979, 1985; Cram & Giampapa 1987; Robinson et al. 1990): No photosperic component in inactive stars; gradually increasing absorption in denser/more active chromospheres, eventually reaching a maximum absoption; finally, as chromospheric column densities rise further, collisions dominate the line formation, and the continuum drops away, the line fills in and goes into emission. In G stars, sufficient chromospheric densities are apparently never achieved for the last stage (D3 emission) to take place, but in K stars (with intrinsically larger chromospheric densities to start) it is possible to fill in D3 (HD 82558) and eventually in the latest K stars, drive it into emission (EQ Vir, CC Eri). The decrease in the local continuum with $T_{\rm eff}$ enhances this effect, making the transition to emission sharper and more pronounced. Still, D3 is apparently a sensitive diagnostic of chromospheric densities in very active stars. One should not, however, rule out the contribution of flares to the "filling-in" process. Coronal X-rays, on the other hand, apparently have only a minor effect on D3 formation in active stars, according to present models (AG; Lanzafame & Byrne 1995).

5. Conclusions and future directions

We have studied the He I D3 line in G and K dwarfs with an extended sample of stars, and compared the flux in D3 with colour, rotation, and fluxes in Ca II HK, C IV (1550 Å), and soft X-rays. Our comparisons with the other activity parameters suggest that the D3 line is an indicator of activity in the upper chromosphere, correlating well with the other activity parameters in the regime $P_{rot} \geq 4$ days. Specifically, we find $F_{\rm D3} \propto \Delta F_{\rm HK}^{1.5\pm0.2}$, $F_{\rm D3} \propto F_{\rm CIV}^{0.7\pm0.1}$, and $F_{\rm D3} \propto \Delta F_{\rm X}^{0.6\pm0.2}$. For late F, G and K stars the D3 absorption shows a colour dependent upper limit, given by log $F_{\rm D3} \approx -2.17(B-V) + 6.54$, or converting to $T_{\rm eff}$, $F_{\rm D3} \approx 2 \times 10^{-30} T_{\rm eff}^{9.27}$ (erg cm^{-2}s^{-1}) for $0.5 \leq B-V \leq 1.2$. This is smaller than current theoretical predictions (AG), thus providing some constraints for models of the D3 line formation. The maximum W_λ in G dwarfs is consistent with the D3 absorption seen in the brightest non-flaring plage on the sun (AG), and improves agreement between 10830 and D3-derived chromospheric filling factors computed by the method outlined by AG. Slower rotators ($P_{\rm rot} \geq 4$ days) show $F_{\rm D3} \propto P_{\rm rot}^{-1.2\pm0.2}$; correlations with Rossby number show more scatter. For faster rotators D3 shows a more divergent behaviour, with observed absorption line fluxes smaller than expected from the trend found for slow rotators. For a few late K stars in our sample the D3 line even shows emission, consistent with the expected chromospheric density increase in the cooler dwarfs, and their reduced continuum levels. Increased low-level flaring may also play a role in "filling-in" D3 in the most active stars.

Our work suggests several potentially fruitful future lines of inquiry. To better define and explore the effect of extreme activity on D3 formation, more observations on rapidly rotating dwarfs ($P_{\rm rot} \leq 3$ days) would be useful, particularly near the G/K boundary where D3 behaviour changes rapidly. This zone of rapid change could be a useful diagnostic of upper chromospheric densities, and thus a good way to test models. Along the same lines, we reiterate the calls for more coordinated measurements of He I 10830Å and D3 (AG), since their strongly coupled formation should also be useful checks for the atmospheric and D3 models. More complete He I atomic models (see Lanzafame & Byrne 1995) and more realistic simulations of the outer atmosphere (see AG) should also be pursued. High S/N, and high time resolution monitoring of D3 in selected active G and K stars would be useful to test how important flares are for D3 formation in active stars, and to explore the use-

fulness of D3 as an optical flare monitor for active stars with bothersomely bright continua. Finally, similar surveys should be undertaken in evolved stars and in M dwarfs. We are actively pursuing several of these observational approaches. Together, these proposed steps should help further understanding of how the He I D3 line is formed, and increase its usefulness as a probe of stellar activity and outer atmospheric structure.

Acknowledgements. This research is supported by the Smithsonian Institution Center Fellowship program (S.S.), and by the exchange program between the Academy of Finland and the USSR Academy of Sciences (J.H.). We gratefully acknowledge ESO for observing time and travel support, J. Andersen for help with some of the observations, and P. Magain for the use of some of his data reduction programs. J.H. and S.S. thank Dr. P. Petrov and the staff of the Crimean Astrophysical Observatory for observing time and their hospitality. S.S. is indebted to I. Tuominen, O. Vilhu and the staff at the Observatory at the University of Helsinki, where part of this work was completed, for their hospitality, support, lakka, piimä, and olut. We have made extensive use of the SIMBAD database, operated at CDS, Strasbourg, France. Finally, we thank O. Vilhu and D. Sasselov for valuable discussions, Y. Filyurin for help with some of the data analysis, and the referee, A. Lanzafame, for his thorough review and helpful suggestions.

References

Allen, C.W., 1973, Astrophysical Quantities, Third Edition. Athlone, London
Andretta, V., Giampapa, M.S. 1995, ApJ 439, 405 (AG)
Athay, R.G., Johnson, H.R: 1960, ApJ 131, 413
Ayres, T.R., Fleming, T.A., Simon, T. et al. 1995, ApJS 96, 223
Baliunas, S.L., Donahue, R.A., Soon, W.H., et al. 1995, ApJ 438, 269
Baliunas, S.L., Sokoloff, D., Soon, W.H. 1996, ApJ 457, L99
Basri, G., Laurent, R., Walter, F.M. 1985 ApJ 298, 761
Berman, L., 1931, Lick. Obs. Bull. 15, 109
Bopp, B.W., Fekel, F.C. 1977, AJ 82, 490
Bookbinder, J.A. 1985, PhD Thesis, Harvard, Univ.
Butler, C.J., Doyle, J.G., Andrews, A.D., Byrne, P.B., Linsky, J.L., Bornmann, P.L., Rodonò, M., Pazzani, V., Simon, T. 1987, A&A 174, 139
Caillault, J.-P., 1982, AJ 87, 558
Cayrel, R., 1988, In: Cayrel de Strobel G., Spite M. (eds.) IAU Symp. 132. Reidel, Dordrecht, p. 345
Cram, L.E., Giampapa, M.S. 1987, ApJ 323, 316
Cram, L.E., Mullan, D.J., 1979, ApJ 234, 579
Cram, L.E., Mullan, D.J., 1985, ApJ 294, 626
Cuntz, M., Luttermoser, D.G. 1990, ApJ 353, L39
Danks, A.C., Lambert, D.L., 1985, A&A 148, 293
Dempsey, R.C., Linsky, J.L., Fleming, T.A., Schmitt, J.H.M.M. 1993, ApJS 86, 599
Donahue, R.A., Saar, S.H., Baliunas, S.L. 1996, ApJ , 466, 384
Duncan, D.K., Vaughan, A.H., Wilson, O.C., et al. 1991, ApJS 76, 383
Garcia López, R.J., Rebolo, R., Beckman, J.E., McKeith, C.D. 1993, A&A 273, 482 (GL)
Giampapa, M.S., Linsky, J.L., Schneeberger, T.J., Worden, S.P., 1978, ApJ 226, 144
Giampapa, M.S., Rosner, R., Kashyap, V., Fleming, T.A., Schmitt, J.H.M.M., Bookbinder, J.A. 1996, ApJ , 463, 707
Gray, D.F., 1988, Lectures on Spectral Line Analysis: F, G, and K Stars. The Publisher. Arva.
Hallam, K.L., Aliner, B., Endal, A.S. 1991, ApJ 372, 610
Harvey, J.W., Livingston, W.C. 1993, In: D.M. Rabin, J.T. Jeffries, & C.A. Lindsey (eds.), IAU Symp. 154, Infrared Solar Physics, Dordrecht, Reidel, 59
Hempelmann, A., Schmitt, J.H.M.M., Schultz, M., Rüdiger, G., Stepieǹ, K. 1995, A&A 294, 515
Hempelmann, A., Schmitt, J.H.M.M., Stepieǹ, K. 1996, A&A 305, 284
Henry, T.J., Soderblom, D.R., Donahue, R.A., Baliunas, S.L. 1996, AJ 111, 439
Hirayama, T. 1971, Sol. Phys. 19, 384
Hooten, J.T., Hall, D.S. 1990, ApJS 74, 225
Huenemoerder, D.P., Ramsey, L.W., 1987, ApJ 319, 392
Huovelin, J., Poutanen, M., Tuominen, I., 1986, In: Urpo S. (ed.) Proc. 1st Finnish-Soviet Symposium on Radio Astronomy, Helsinki Univ. of Technology Radio Lab. Report S166. Helsinki, p. 3
Innis, J.L., Thompson, K., Coates, D.W., Lloyd Evans, T. 1989, MNRAS 235, 1411
Johnson, H.M. 1986, ApJ 303, 470
Jetsu, L. 1993, A&A 276, 345
Kim, Y.-C., Demarque, P. 1996, ApJ 457, 340
Kurucz, R. L. 1992, Rev. Mex. Astron. Astrof. 23, 45
Lambert, D.L., O'Brien, G.T., 1983, A&A 128, 110
Landman, D.A., 1981, ApJ 244, 345
Lanzafame, A.C., Byrne, P.B. 1995, A&A 303, 155
Lloyd-Evans, T., Koen, M.C.J. 1987, SAAO Circ. 11, 21
Linsky, J.L., Andrulis, C., Saar, S.H., Ayres, T.R., Giampapa, M.S. 1994, In: J.-P. Caillault (ed.), Cool Stars, Stellar Systems, and the Sun, ASP. Conf. Ser. 64, 438
Maggio, A., Sciortino, S. Vaiana, G.S., Majer, P., Bookbinder, J., Golub, L., Harnden, Jr., F.R., Rosner, R. 1987, ApJ 315, 867
Marcy, G.W., 1984, ApJ 276, 286
Milkey, R.W., Heasley, J.N., Beebe, H.A. 1973, ApJ 186, 1043
Moore, C.E., Minnaert, G.J., Houtgast, J. 1966, The Solar Spectrum 2935Å to 8770 Å, NBS Monograph 61
O'Brien, G.T., 1980, unpublished Ph.D. thesis, Univ. of Texas
Olah, K., Pettersen, B.R., 1991, A&A 242, 443
Ossendrijver, A.J.H. 1996, A&A , submitted
Noyes, R.W., Hartmann, L.W., Baliunas, S.L., Duncan, D.K., Vaughan, A.H., 1984, ApJ 279, 763
Pasquini, L., Pallavicini, R., 1991, A&A 251, 199
Pasquini, L., Pallavicini, R., Pakull, M., 1988, A&A 191, 253
Pettersen, B.R., 1989, A&A 209, 279
Pettersen, B.R., Coleman, L.A., 1981, ApJ 251, 571
Pettersen, B.R., Evans, D.S., Coleman, L.A., 1984, ApJ 282, 214
Piskunov, N., Huenemoerder, D.P., Saar, S.H. 1994, In: J.-P. Caillault (ed.), Cool Stars, Stellar Systems, and the Sun, ASP. Conf. Ser. 64, 661
Robinson, C.R., Bopp, B.W., 1987, In: Linsky J.L., Stencel R.E. (eds.) Cool Stars, Stellar Systems and the Sun. Springer, New York, p. 509
Robinson, R.D., Cram, L.W., Giampapa, M.S. 1990, ApJS 74, 891
Rutten, R., 1987a, A&A 177, 131
Rutten, R., 1987b, Ph.D. Thesis, Univ. of Utrecht
Rutten, R., Schrijver, C.J., Lemmens, A.F.P., Zwaan, C., 1991, A&A 252, 203
Rutten, R., Schrijver, C.J., Zwaan, C., Duncan, D.K., Mewe, R. 1989, A&A 219, 239
Saar, S.H., Golub, L., Bopp, B.W., Herbst, W., Huovelin, J. 1990b, In: E. Rolfe (ed.), Evolution in Astrophysics: IUE Astronomy in the Era of New Space Missions, ESA SP–310, 168

Saar, S.H., Huovelin, J., Shcherbakov, A.G., Gustafsson, B., Andersen, J. 1988, BAAS 20, 997
Saar, S.H., Nordström, B., Andersen, J., 1990a, A&A , 235, 291
Saar, S.H., Osten, R.A., 1997, MNRAS , 284, 803
Schrijver, C.J., 1995, A&ARev 6, 181
Shine, R., Gerola, H., Linsky, J.L. 1975, ApJ 202, L101
Soderblom, D.R., 1985, AJ 90, 2103
Soderblom, D.R., Clements, S.D. 1987, AJ 93, 920
Stocke, J.T., Morris, S.L., Gioia, M., Maccacaro, T., Schild, R., Wolter, A., Fleming, T.A., Henry, J.P., 1991, ApJS 76, 813
Strassmeier, K.G., Fekel, F.C., Bopp, B.W., Dempsey, R.C., Henry, G.W. 1990, ApJS 72, 191
Torres, C.A.O., Ferraz Mello, S. 1973, A&A 27, 331
Vilhu, O., 1984, A&A 133, 117
Vilhu, O., Gustafsson, B., Walter, F.M. 1989, A&A 241, 167
Wolff, S.C., Boesgaard, A.M., Simon, T., 1986, ApJ 310, 360
Wolff, S.C., Heasley, J.N., 1984, PASP 96, 231
Wolff, S.C., Heasley, J.N., 1987, PASP 99, 957
Wolff, S.C., Heasley, J.N., Varsik, J. 1985, PASP 97, 707
Wood, B.E., Brown, A., Linsky, J.L., Kellett, B.J., Bromage, B.E., Hodgkin, S.T., Pye, J.P. 1994, ApJS 93, 287
Zirin, H. 1975, ApJ 199, L63

This article was processed by the author using Springer-Verlag LaTeX A&A style file *L-AA* version 3.